



GLOBAL JOURNAL OF RESEARCHES IN ENGINEERING: F
ELECTRICAL AND ELECTRONICS ENGINEERING
Volume 17 Issue 5 Version 1.0 Year 2017
Type: Double Blind Peer Reviewed International Research Journal
Publisher: Global Journals Inc. (USA)
Online ISSN: 2249-4596 & Print ISSN: 0975-5861

Optimal Power Flow using a hybrid Particle Swarm Optimizer with Moth Flame Optimizer

By Pradeep Jangir, Siddharth A. Parmar, Indrajit N. Trivedi & Arpita

Sri Ganganagar College of Ayurvedic Science

Abstract- In this work, the most common problem of the modern power system named optimal power flow (OPF) is optimized using the novel hybrid meta-heuristic optimization algorithm Particle Swarm Optimization-Moth Flame Optimizer (HPSO-MFO) method. Hybrid PSO-MFO is a combination of PSO used for exploitation phase and MFO for exploration phase in an uncertain environment. Position and Speed of particle are reorganized according to Moth and flame location in each iteration. The hybrid PSO-MFO method has a fast convergence rate due to the use of roulette wheel selection method. For the OPF solution, standard IEEE-30 bus test system is used. The hybrid PSO-MFO method is implemented to solve the proposed problem. The problems considered in the OPF are fuel cost reduction, Voltage profile improvement, Voltage stability enhancement, Active power loss minimization and Reactive power loss minimization. The results obtained with hybrid PSO-MFO method is compared with other techniques such as Particle Swarm Optimization (PSO) and Moth Flame Optimizer (MFO).

Keywords: *optimal power flow; voltage stability; power system; hybrid PSO-MFO; constraints.*

GJRE-F Classification: FOR Code: 090699



Strictly as per the compliance and regulations of:



© 2017. Pradeep Jangir, Siddharth A. Parmar, Indrajit N. Trivedi & Arpita. This is a research/review paper, distributed under the terms of the Creative Commons Attribution-Noncommercial 3.0 Unported License (<http://creativecommons.org/licenses/by-nc/3.0/>), permitting all non commercial use, distribution, and reproduction in any medium, provided the original work is properly cited.

Optimal Power Flow using a hybrid Particle Swarm Optimizer with Moth Flame Optimizer

Pradeep Jangir ^α, Siddharth A. Parmar ^σ, Indrajit N. Trivedi ^ρ & Arpita ^ω

Abstract- In this work, the most common problem of the modern power system named optimal power flow (OPF) is optimized using the novel hybrid meta-heuristic optimization algorithm Particle Swarm Optimization-Moth Flame Optimizer (HPSO-MFO) method. Hybrid PSO-MFO is a combination of PSO used for exploitation phase and MFO for exploration phase in an uncertain environment. Position and Speed of particle are reorganized according to Moth and flame location in each iteration. The hybrid PSO-MFO method has a fast convergence rate due to the use of roulette wheel selection method. For the OPF solution, standard IEEE-30 bus test system is used. The hybrid PSO-MFO method is implemented to solve the proposed problem. The problems considered in the OPF are fuel cost reduction, Voltage profile improvement, Voltage stability enhancement, Active power loss minimization and Reactive power loss minimization. The results obtained with hybrid PSO-MFO method is compared with other techniques such as Particle Swarm Optimization (PSO) and Moth Flame Optimizer (MFO). Results show that hybrid PSO-MFO gives better optimization values as compared with PSO and MFO which verifies the effectiveness of the suggested algorithm.

Keywords: optimal power flow; voltage stability; power system; hybrid PSO-MFO; constraints.

I. INTRODUCTION

At the present time, The Optimal power flow (OPF) is a very significant problem and most focused objective for power system planning and operation [1]. The OPF is the elementary tool which permits the utilities to identify the economic operational and secure states in the system [2]. The OPF problem is one of the utmost operating desires of the electrical power system [3]. The prior function of OPF problem is to evaluate the optimum operational state for Bus system by minimizing each objective function within the limits of the operational constraints like equality constraints and inequality constraints [4]. Hence, the optimal power flow problem can be defined as an extremely non-linear and non-convex multimodal optimization problem [5].

From the past few years too many optimization techniques were used for the solution of the Optimal Power Flow (OPF) problem. Some traditional methods

used to solve the proposed problem have some limitations like converging at local optima and so they are not suitable for binary or integer problems or to deal with the lack of convexity, differentiability, and continuity [6]. Hence, these techniques are not suitable for the actual OPF situation. All these limitations are overcome by metaheuristic optimization methods. Some of these methods are [7-10]: genetic algorithm (GA) [11], hybrid genetic algorithm (HGA) [12], enhanced genetic algorithm (EGA) [13-14], differential evolution algorithm (DEA) [15-16], artificial neural network (ANN) [17], particle swarm optimization algorithm (PSO) [18], tabu search algorithm (TSA) [19], gravitational search algorithm (GSA) [20], biogeography based optimization (BBO) [21], harmony search algorithm (HSA) [22], krill herd algorithm (KHA) [23], cuckoo search algorithm (CSA) [24], ant colony algorithm (ACO) [25], bat optimization algorithm (BOA) [26], Ant-lion optimizer (ALO) [27-28] and Multi-Verse optimizer (MVO) [29].

In the present work, a newly introduced hybrid meta-heuristic optimization technique named Hybrid Particle Swarm Optimization-Moth Flame Optimizer (HPSO-MFO) is applied to solve the Optimal Power Flow problem. HPSO-MFO comprises of best characteristic of both Particle Swarm Optimization [30] and Moth-Flame Optimizer [31-32] algorithm. The capabilities of HPSO-MFO are finding the global solution, fast convergence rate due to the use of roulette wheel selection, can handle continuous and discrete optimization problems.

According to No Free Lunch Theorem [27,29,30], particular meta-heuristic algorithm is not best for every problem. So, we considered HPSO-MFO for continuous optimal power flow problem based on No Free Lunch Theorem. In this work, the HPSO-MFO is presented to standard IEEE-30 bus test system [33] to solve the OPF [34-37] problem. There are five objective cases considered in this paper that have to be optimized using HPSO-MFO technique are Fuel Cost Reduction, Voltage Stability Improvement, Voltage Deviation Minimization, Active Power Loss Minimization and Reactive Power Loss Minimization. The results show the optimal adjustments of control variables in accordance with their limits. The results obtained using HPSO-MFO technique has been compared with Particle Swarm Optimization (PSO) and Moth Flame Optimizer (MFO) techniques. The results show that HPSO-MFO gives better optimization values as compared to other

Author ^α σ: L.E. College, Morbi (Gujarat) India.
e-mails: pkjmttech@gmail.com, saparmar92@gmail.com

Author ^ρ: G.E. College, Gandhinagar (Gujarat) India.
e-mail: forumtrivedi@gmail.com

Author ^ω: Sri Ganganagar College of Ayurvedic Science & Hospital, Sri Ganganagar (Rajasthan) India. e-mail: apyjangid@gmail.com

methods which prove the effectiveness of the proposed algorithm.

This paper is summarized as follow: After the first section of the introduction, the second section concentrates on concepts and key steps of standard PSO and MFO techniques and the proposed Hybrid PSO-MFO technique. The third section presents the formulation of Optimal Power Flow problem. Next, we apply HPSO-MFO to solve OPF problem on IEEE-30 bus system in order to optimize the operating conditions of the power system. Finally, the results and conclusion are drawn in the last section.

II. STANDARD PSO AND STANDARD MFO

a) Particle Swarm Optimization

The particle swarm optimization algorithm (PSO) was discovered by James Kennedy and Russell C. Eberhart in 1995 [30]. This algorithm is inspired by the simulation of social psychological expression of birds and fishes. PSO includes two terms P_{best} and G_{best} . Position and velocity are updated over the course of iteration from these mathematical equations:

$$v_{ij}^{t+1} = wv_{ij}^t + c_1R_1(Pbest^t - X^t) + c_2R_2(Gbest^t - X^t) \quad (1)$$

$$X^{t+1} = X^t + v^{t+1} \quad (i = 1, 2...NP) \text{ And } (j = 1, 2...NG) \quad (2)$$

Where

$$w = w^{\max} - \frac{(w^{\max} - w^{\min}) * iteration}{\max iteration}, \quad (3)$$

$w^{\max} = 0.4$ and $w^{\min} = 0.9$.

v_{ij}^t, v_{ij}^{t+1} is the velocity of aj^{th} member of anth particle at iteration number (t) and ($t+1$). (Usually $C_1=C_2=2$), r_1 and r_2 Random number (0, 1).

b) Moth-Flame Optimizer

A novel nature-inspired Moth-Flame optimization algorithm [31] based on the transverse orientation of Moths in space. Transverse orientation for navigation uses a constant angle by Moths with respect to Moon to fly in straight direction in night. In MFO algorithm that Moths fly around flames in a Logarithmic spiral way and finally converges towards the flame. Spiral way expresses the exploration area and it guarantees to exploit the optimum solution [31]:

Moth-Flame optimizer is first introduced by Seyedali Mirjalili in 2015 [31]. MFO is a population - based algorithm; we represent the set of moths in a matrix:

$$M = \begin{bmatrix} m_{1,1} & m_{1,2} & \dots & m_{1,d} \\ m_{2,1} & m_{2,2} & \dots & m_{2,d} \\ \vdots & \vdots & \ddots & \vdots \\ \vdots & \vdots & \ddots & \vdots \\ m_{n,1} & m_{n,2} & \dots & m_{n,d} \end{bmatrix} \quad (4)$$

Where n represents a number of moths and d represents a number of variables (dimension).

For all the moths, we also assume that there is an array for storing the corresponding fitness values as follows:

$$OM = \begin{bmatrix} OM_1 \\ OM_2 \\ \vdots \\ OM_n \end{bmatrix} \quad (5)$$

Where n is the number of moths.

Note that the fitness value is the return value of the fitness (objective) function for each moth. The position vector (first row in the matrix M for instance) of each moth is passed to the fitness function and the output of the fitness function is assigned to the corresponding moth as its fitness function (OM_i in the matrix OM for instance).

Other key components in the proposed algorithm are flames. We consider a matrix similar to the moth matrix [31]:

$$F = \begin{bmatrix} FL_{1,1} & FL_{1,2} & \dots & FL_{1,d} \\ FL_{2,1} & FL_{2,2} & \dots & FL_{2,d} \\ \vdots & \vdots & \ddots & \vdots \\ \vdots & \vdots & \ddots & \vdots \\ FL_{n,1} & FL_{n,2} & \dots & FL_{n,d} \end{bmatrix} \quad (6)$$

Where n shows a number of moths and d represents a number of variables (dimension).

We know that the dimension of M and F arrays are equal. For the flames, we also assume that there is an array for storing the corresponding fitness values [31]:

$$OF = \begin{bmatrix} OFL_1 \\ OFL_2 \\ \vdots \\ OFL_n \end{bmatrix} \quad (7)$$

Where n is the number of moths.

Here, it must be noted that moths and flames both are solutions. The variance among them is the manner we treat and update them, in the iteration. The moths are genuine search agents that move all over the search space while flames are the finest location of moths that achieves so far. Therefore, every moth searches around a flame and updates it in the case of discovering an enhanced solution. With this mechanism, a moth never loses its best solution.

The MFO algorithm is three rows that approximate the global solution of the problems defined like as follows [31]:

$$\text{MFO} = (\mathbf{I}, \mathbf{P}, \mathbf{T}) \tag{8}$$

I is the function that yields an uncertain population of moths and corresponding fitness values. The methodical model of this function is as follows:

$$I : \phi \rightarrow \{M, OM\} \tag{9}$$

The P function, which is the main function, expresses the moths all over the search space. This function receives the matrix of M and takes back its updated one at every time with each iteration.

$$P : M \rightarrow M \tag{10}$$

The T returns true and false according to the termination Criterion satisfaction:

$$T : M \rightarrow \{true, false\} \tag{11}$$

In order to mathematical model this behavior, we change the location of each Moth regarding a flame with the following equation:

$$M_i = S(M_i, F_j) \tag{12}$$

Where M_i indicate the i^{th} moth, F_j indicates the j^{th} flame and S is the spiral function.

In this equation flame $FL_{n,d}(\text{search agent} * \text{dimension})$ of equation (6) modifies the moth matrix of equation (12).

Considering these points, we define a log (logarithmic scale) spiral for the MFO algorithm as follows [31]:

$$S(M_i, F_j) = D_i * e^{bt} \cos(2\pi t) + F_j \tag{13}$$

Where: D_i expresses the distance of the moth for the j^{th} flame, b is a constant for expressing the shape of the log (logarithmic) spiral, and t is a random value in $[-1, 1]$.

$$D_i = |F_j - M_i| \tag{14}$$

Where: M_i represent the i^{th} moth, F_j represents the j^{th} flame, and where D_i expresses the path length of the i^{th} moth for the j^{th} flame.

The no. of flames are adaptively reduced with the iterations. We use the following formulation:

$$\text{flame no} = \text{round}\left(N - l * \frac{N - 1}{T}\right) \tag{15}$$

Where l is the present number of iteration, N is the maximum number of flames, and T shows the maximum number of iterations.

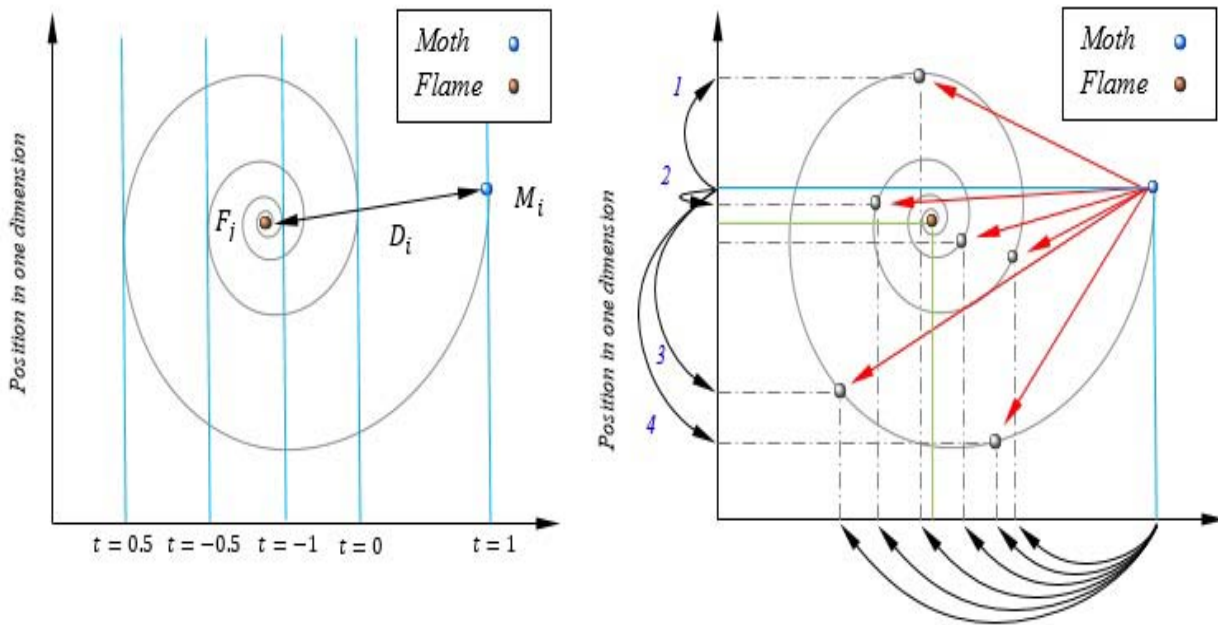


Fig. 1: A conceptual model of position updating of a moth around a flame

We utilize Quick sort algorithm, the sorting is in the $O(n \log n)$ best and $O(n^2)$ worst condition,

respectively. Considering the P function, so, total computational complexity is defined as follows:

$$O(MFO) = O(t(O(\text{Quick sort}) + O(\text{position update}))) \quad O(MFO) = O(t(n^2 + n * d)) = O(tn^2 + tnd) \quad (16)$$

Where n shows a number of moths, t represents maximum no. of iterations, and d represents no. of variables.

c) The Hybrid PSO-MFO Algorithm

The drawback of PSO is the limitation to cover small search space while solving higher order or complex design problem due to constant inertia weight. This problem can be tackled with Hybrid PSO-MFO as it extracts the quality characteristics of both PSO and MFO. Moth-Flame Optimizer is used for exploration phase as it uses logarithmic spiral function so it covers a broader area in uncertain search space. Because both of the algorithms are randomization techniques so we use term uncertain search space during the computation over the course of iteration from starting to maximum iteration limit. Exploration phase means the capability of an algorithm to try out a large number of possible solutions. The position of particle that is

responsible for finding the optimum solution to the complex non-linear problem is replaced with the position of Moths that is equivalent to the position of the particle but highly efficient to move solution towards optimal one. MFO directs the particles faster towards optimal value, reduces computational time. As we know that that PSO is a well-known algorithm that exploits the best possible solution for its unknown search space. So the combination of best characteristic (exploration with MFO and exploitation with PSO) guarantees to obtain the best possible optimal solution of the problem that also avoids local stagnation or local optima of the problem.

A set of Hybrid PSO-MFO is the combination of separate PSO and MFO. Hybrid PSO-MFO merges the best strength of both PSO in exploitation and MFO in exploration phase towards the targeted optimum solution.

$$v_{ij}^{t+1} = wv_{ij}^t + c_1R_1(\text{Moth_Pos}^t - X^t) + c_2R_2(\text{Gbest}^t - X^t) \quad (17)$$

III. OPTIMAL POWER FLOW PROBLEM FORMULATION

As specified before, OPF is the optimized problem of power flow that provides the optimum values

of independent variables by optimizing a predefined objective function with respect to the operating bounds of the system [1]. The OPF problem can be mathematically expressed as a non-linear constrained optimization problem as follows [1]:

$$\text{Minimize } f(a,b) \quad (18)$$

$$\text{Subject to } s(a,b)=0 \quad (19)$$

$$\text{And } h(a,b)\leq 0 \quad (20)$$

Where, a =vector of state variables, b =vector of control variables, $f(a,b)$ =objective function, $s(a,b)$ =different equality constraints set, $h(a,b)$ =different inequality constraints set.

The evaluation function for the OPF problem is given as follows:

$$\text{Evaluation Function} = \text{Search Agents} * \text{Maximum Iterations} = 40*500 = 20000$$

a) Variables

i. Control variables

The control variables should be adjusted to fulfill the power flow equations. For the OPF problem, the set for control variables can be formulated as [1], [4]:

$$b^T = [P_{G_2} \dots P_{G_{N_{Gen}}}, V_{G_1} \dots V_{G_{N_{Gen}}}, Q_{C_1} \dots Q_{C_{N_{Com}}}, T_1 \dots T_{N_{Tr}}] \quad (21)$$

Where,

P_G = Real power output at the PV(Generator) buses excluding at the slack (Reference) bus.

V_G = Magnitude of Voltage at PV (Generator) buses.

Q_C = shunt VAR compensation.

T = tap settings of the transformer.

N_{Gen} , N_{Tr} , N_{Com} = No. of generator units, No. of tap changing transformers and No. of shunt VAR compensation devices, respectively.

The control variables are the decision variables of the power system which could be adjusted as per the requirement.

ii. State variables

There is a need of variables for all OPF formulations for the characterization of the Electrical Power Engineering state of the system. So, the state variables can be formulated as [1], [4]:

$$a^T = [P_{G_1}, V_{L_1} \dots V_{L_{NLB}}, Q_{G_1} \dots Q_{G_{N_{Gen}}}, S_{L_1} \dots S_{L_{N_{Line}}}] \quad (22)$$

Where,

P_{G_1} = Real power generation at reference bus.

V_L = Magnitude of Voltage at Loadbuses.

Q_G = Reactive power generation of all generators.

S_l = Transmission line loading.

NLB , $Nline$ = No. of PQ buses and the No. of transmission lines, respectively.

b) Constraints

There are two OPF constraints named inequality and equality constraints. These constraints are explained in the sections given below.

i. Equality constraints

The physical condition of the power system is described by the equality constraints of the system. These equality constraints are basically the power flow equations which can be explained as follows [1], [4].

a. Real power constraints

The real power constraints can be formulated as follows:

$$P_{Gi} - P_{Di} - V_i \sum_{j=1}^{NB} V_j [G_{ij} \cos(\delta_{ij}) + B_{ij} \sin(\delta_{ij})] = 0 \quad (23)$$

b. Reactive power constraints

The reactive power constraints can be formulated as follows:

$$Q_{Gi} - Q_{Di} - V_i \sum_{j=1}^{NB} V_j [G_{ij} \sin(\delta_{ij}) - B_{ij} \cos(\delta_{ij})] = 0 \quad (24)$$

Where, $\delta_{ij} = \delta_i - \delta_j$ is the phase angle of voltage between buses i and j. NB = total No. of buses, P_G = real power output, Q_G = reactive power output, P_D = active power load demand, Q_D = reactive power load demand, B_{ij} and G_{ij} = elements of the admittance matrix $Y_{ij} = (G_{ij} + jB_{ij})$ shows the susceptance and conductance between bus i and j, respectively, Y_{ij} is the mutual admittance between buses i and j.

ii. Inequality constraints

The boundaries of power system devices together with the bounds created to surety system security are given by inequality constraints of the OPF [4], [5].

a. Generator constraints

For all generating units including the reference bus: voltage magnitude, real power and reactive power

outputs should be constrained within its minimum and maximum bounds as given below [27]:

$$V_{G_i}^{lower} \leq V_{G_i} \leq V_{G_i}^{upper}, i=1, \dots, NGen \quad (25)$$

$$P_{G_i}^{lower} \leq P_{G_i} \leq P_{G_i}^{upper}, i=1, \dots, NGen \quad (26)$$

$$Q_{G_i}^{lower} \leq Q_{G_i} \leq Q_{G_i}^{upper}, i=1, \dots, NGen \quad (27)$$

b. Transformer constraints

Tap settings of transformer should be constrained inside their stated minimum and maximum bounds as follows [27]:

$$T_{G_i}^{lower} \leq T_{G_i} \leq T_{G_i}^{upper}, i=1, \dots, NGen \quad (28)$$

c. Shunt VAR compensator constraints

Shunt VAR compensation devices need to be constrained within its minimum and maximum bounds as given below [27]:

$$Q_{C_i}^{lower} \leq Q_{C_i} \leq Q_{C_i}^{upper}, i=1, \dots, NGen \quad (29)$$

d. Security constraints

These comprise the limits of a magnitude of the voltage at PQ buses and loadings on the transmission line. Voltage for every PQ bus should be limited by their minimum and maximum operational bounds. Line flow over each line should not exceed its maximum loading limit. So, these limitations can be mathematically expressed as follows [27]:

$$V_{L_i}^{lower} \leq V_{L_i} \leq V_{L_i}^{upper}, i=1, \dots, NGen \quad (30)$$

$$S_{l_i} \leq S_{l_i}^{upper}, i=1, \dots, Nline \quad (31)$$

The control variables are self-constraint. The inequality constrained of state variables comprises the magnitude of PQ bus voltage, active power production at reference bus, reactive power production and loadings on line may be encompassed into an objective function in terms of quadratic penalty terms. In which, the penalty factor is multiplied by the square of the indifference value of state variables and is included in the objective function and any impractical result achieved is declined [27].

Penalty function may be mathematically formulated as follows:

$$J_{aug} = J + \partial_P (P_{G_1} - P_{G_1}^{lim})^2 + \partial_V \sum_{i=1}^{NLB} (V_{L_i} - V_{L_i}^{lim})^2 + \partial_Q \sum_{i=1}^{NGen} + \partial_S \sum_{i=0}^{Nline} (S_{l_i} - S_{l_i}^{max})^2 \quad (32)$$

Where, $\partial_P, \partial_V, \partial_Q, \partial_S$ = penalty factors

U_{lim} = Boundary value of the state variable U.

If U is greater than the maximum limit, U_{lim} takings the value of this one, if U is lesser than the

minimum limit U_{lim} taking the value of that limit. This can be shown as follows [27]:

$$U^{lim} = \begin{cases} U^{upper} & ; U > U^{upper} \\ U^{lower} & ; U < U^{lower} \end{cases} \quad (33)$$

IV. APPLICATION AND RESULTS

The PSO-MFO technique has been implemented for the OPF solution for standard IEEE 30-bus test system and for a number of cases with dissimilar objective functions. The used software program is written in MATLAB R2014b computing surroundings and used on a 2.60 GHz i5 PC with 4 GB RAM. In this work the HPSO-MFO population size is selected to be 40.

a) IEEE 30-bus test system

With the purpose of elucidating the strength of the suggested HPSO-MFO technique, it has been verified on the standard IEEE 30-bus test system as displays in fig. 2. The standard IEEE 30-bus test system selected in this work has the following features[6], [33]: NGen = No. of generators = 6 at buses 1,2,5,8,11 and 13, NTr = No. of regulating transformers having off-nominal tap ratio = 4 between buses 4-12, 6-9, 6-10 and 28-27, NCom = No. of shunt VAR Compensators = 9 at buses 10,12,15,17,20,21,23,24 and 29 and NLB = No. of load buses = 24.

In addition, generator cost coefficient data, the line data, bus data, and the upper and lower bounds for the control variables are specified in [33].

In given test system, five diverse cases have been considered for various purposes and all the acquired outcomes are given in Tables 3, 5, 7, 9, 11. The very first column of this tables denotes the optimal values of control variables found where:

- P_{G1} through P_{G6} and V_{G1} through V_{G6} signifies the power and voltages of generator 1 to generator 6.
- T_{4-12} , T_{6-9} , T_{6-10} and T_{28-27} are the transformer tap settings comprised between buses 4-12, 6-9, 6-10 and 28-27.
- Q_{C10} , Q_{C12} , Q_{C15} , Q_{C17} , Q_{C20} , Q_{C21} , Q_{C23} , Q_{C24} and Q_{C29} denote the shunt VAR compensators coupled at buses 10, 12, 15, 17, 20, 21, 23, 24 and 29.

Further, fuel cost ($\$/hr$), real power losses (MW), reactive power losses ($MVAR$), voltage deviation and L_{max} represent the total generation fuel cost of the system, the total real power losses, the total reactive power losses, the load voltages deviation from 1 and the stability index, respectively. Other particulars for these outcomes will be specified in the next sections.

The control parameters for HPSO-MFO, MFO, PSO used in this problem are given in table 1.

In table 1, no. of variables (dim) shows the six no. of generators used in the 30 bus system. It gives the optimization values for different cases as they depends on the decision variables. In all 5 cases, results are the average value obtained after 10 number of runs.

Table 1: Control parameters used in PSO-MFO, MFO and PSO

Sr. No.	Parameters	Value
1	Population (No. of Search agents) (N)	40
2	Maximum iterations count (t)	500
3	No. of Variables (dim)	25
4	Random Number	[0,1]
5	source acceleration coefficient (c_1 , c_2)	2
6	weighting function (w)	0.65

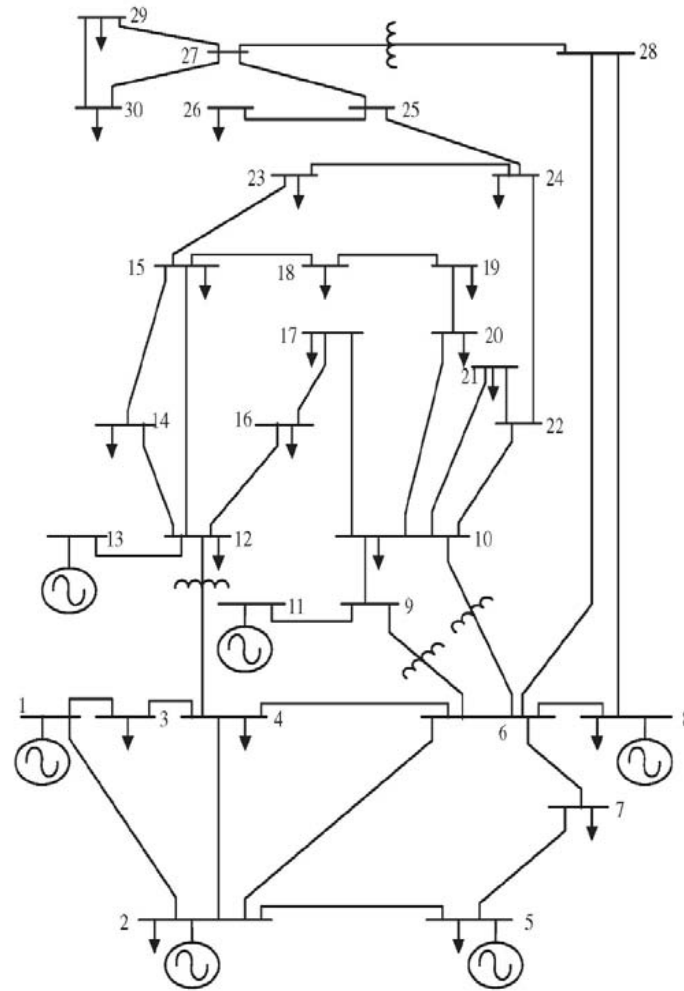


Fig. 2: Single line diagram of IEEE 30-bus test system

Case 1: Minimization of generation fuel cost.

The very common OPF objective that is generation fuel cost reduction is considered in the case 1. Therefore, the objective function Y indicates the complete fuel cost of total generating units and it is calculated by following equation [1]:

$$Y = \sum_{i=1}^{N_{Gen}} f_i (\$/hr) \quad (34)$$

Where, f_i is the total fuel cost of i^{th} generator.

f_i , may be formulated as follow:

$$f_i = u_i + v_i P_{Gi} + w_i P_{Gi}^2 (\$/hr) \quad (35)$$

Where, u_i , v_i and w_i are the simple, the linear and the quadratic cost coefficients of the i^{th} generator, respectively. The cost coefficients values are specified in [33].

The variation of the total fuel cost with different algorithms over iterations is presented in fig. 2. It

demonstrates that the suggested method has outstanding convergence characteristics. The comparison of fuel cost obtained with different methods is shown in table 2 which displays that the results obtained by PSO-MFO are better than the other methods. The optimal values of control variables obtained by different algorithms for case 1 are specified in Table 3. By means of the same settings i.e. control variables boundaries, initial conditions and system data, the results achieved in case 1 with the PSO-MFO technique are compared to some other methods and it display that the total fuel cost is greatly reduced compared to the initial case [6]. Quantitatively, it is reduced from 901.951\$/hr to 799.056\$/hr.

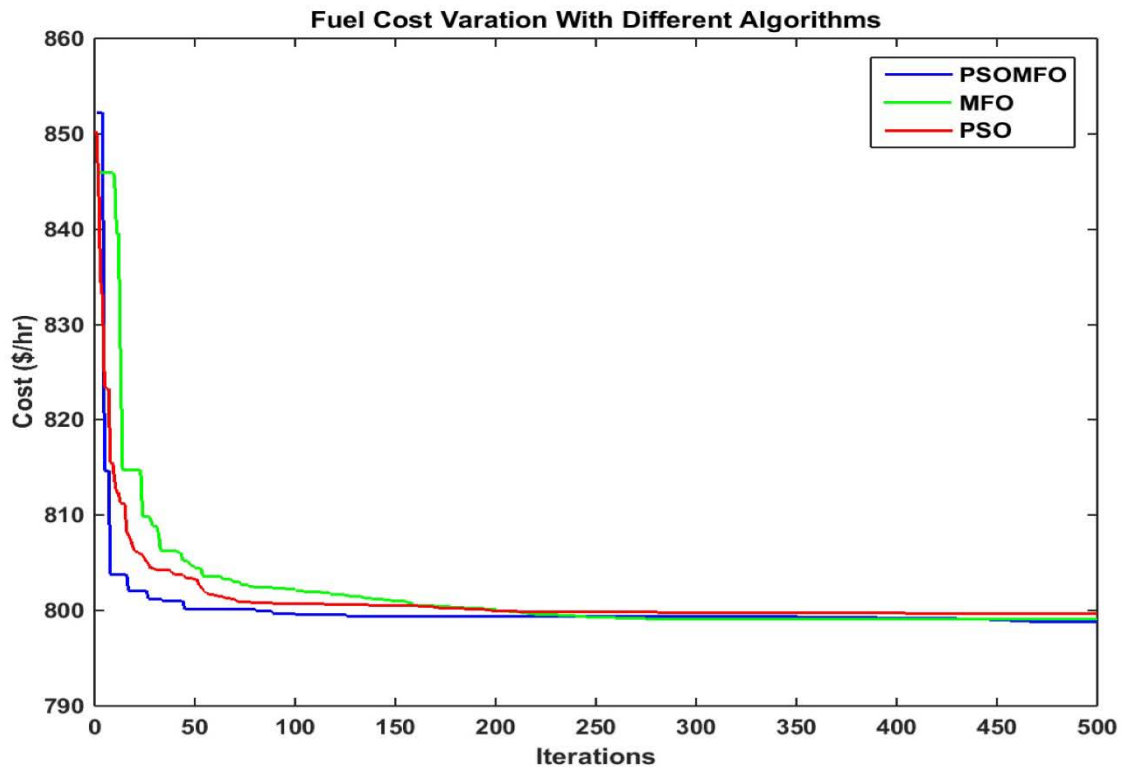


Fig. 3: Fuel cost variations with different algorithms

Table 2: Comparison of fuel cost obtained with different algorithms

Method	Fuel Cost (\$/hr)	Method Description
HPSO-MFO	799.056	Hybrid Particle Swarm Optimization-Moth Flame Optimizer
MFO	799.072	Moth Flame Optimizer
PSO	799.704	Particle Swarm Optimization
DE	799.289	Differential Evolution [15]
BHBO	799.921	Black Hole-Based Optimization [6]

Table 3: Optimal values of control variables for case 1 with different algorithms

Control Variable	Min	Max	Initial	HPSO-MFO	MFO	PSO
P_{G1}	50	200	99.2230	178.133	177.055	177.105
P_{G2}	20	80	80	48.956	48.698	48.748
P_{G5}	15	50	50	21.385	21.304	21.318
P_{G8}	10	35	20	21.706	21.084	20.986
P_{G11}	10	30	20	10.000	11.883	12.049
P_{G13}	12	40	20	12.000	12.000	12.000
V_{G1}	0.95	1.1	1.05	1.100	1.100	1.100
V_{G2}	0.95	1.1	1.04	1.088	1.088	1.088
V_{G5}	0.95	1.1	1.01	1.062	1.062	1.061
V_{G8}	0.95	1.1	1.01	1.070	1.069	1.070
V_{G11}	0.95	1.1	1.05	1.100	1.100	1.100
V_{G13}	0.95	1.1	1.05	1.100	1.100	1.100
T_{4-12}	0	1.1	1.078	0.939	1.044	0.976
T_{6-9}	0	1.1	1.069	1.100	0.900	0.975

T_{6-10}	0	1.1	1.032	1.021	0.985	1.015
T_{28-27}	0	1.1	1.068	0.978	0.965	0.966
QC_{10}	0	5	0	5.000	5.000	2.353
QC_{12}	0	5	0	5.000	5.000	5.000
QC_{15}	0	5	0	5.000	5.000	0.000
QC_{17}	0	5	0	5.000	5.000	0.689
QC_{20}	0	5	0	5.000	5.000	0.003
QC_{21}	0	5	0	5.000	5.000	5.000
QC_{23}	0	5	0	5.000	4.999	0.000
QC_{24}	0	5	0	0.000	5.000	0.000
QC_{29}	0	5	0	3.033	2.725	0.000
Fuel Cost(\$/hr)	-	-	901.951	799.056	799.072	799.704

Case 2: Voltage profile improvement

Bus voltage is considered as most essential and important security and service excellence indices [6]. Here the goal is to reduce the fuel cost and increase voltage profile simultaneously by reducing the voltage deviation of PQ (load) buses from the unity 1.0 p.u.

Hence, the objective function may be formulated by following equation [4]:

$$Y = Y_{\text{cost}} + wY_{\text{voltage-deviation}} \quad (36)$$

Where, w is an appropriate weighting factor, to be chosen by the user to offer a weight or importance to each one of the two terms of the objective function.

Y_{cost} and $Y_{\text{voltage-deviation}}$ are specified as follows [4]:

$$Y_{\text{cost}} = \sum_{i=1}^{NGen} f_i \quad (37)$$

$$Y_{\text{voltage_deviation}} = \sum_{i=1}^{NGen} |V_i - 1.0| \quad (38)$$

The variation of voltage deviation with different algorithms over iterations is sketched in fig. 3. It demonstrates that the suggested method has good convergence characteristics. The statistical values of voltage deviation obtained with different methods are shown in table 4 which display that the results obtained by PSO-MFO are better than the other methods excluding GSA method. The optimal values of control variables obtained by different algorithms for case 2 are specified in Table 5. By means of the same settings the results achieved in case 2 with the PSO-MFO technique are compared to some other methods and it display that the voltage deviation is greatly reduced compared to the initial case [6]. It has been made known that the voltage deviation is reduced from 1.1496 p.u. to 0.1056p.u. using PSO-MFO technique. GSA [2] gives better result than the HPSO-MFO method only in case of voltage deviation among five cases. Due to No Free Lunch (NFL) theorem proves that no one can propose an algorithm for solving all optimization problems. This

means that the success of an algorithm in solving a specific set of problems does not guarantee solving all optimization problems with different type and nature. NFL makes this field of study highly active which results in enhancing current approaches and proposing new meta-heuristics every year. This also motivates our attempts to develop a new Hybrid meta-heuristic for solving OPF Problem.

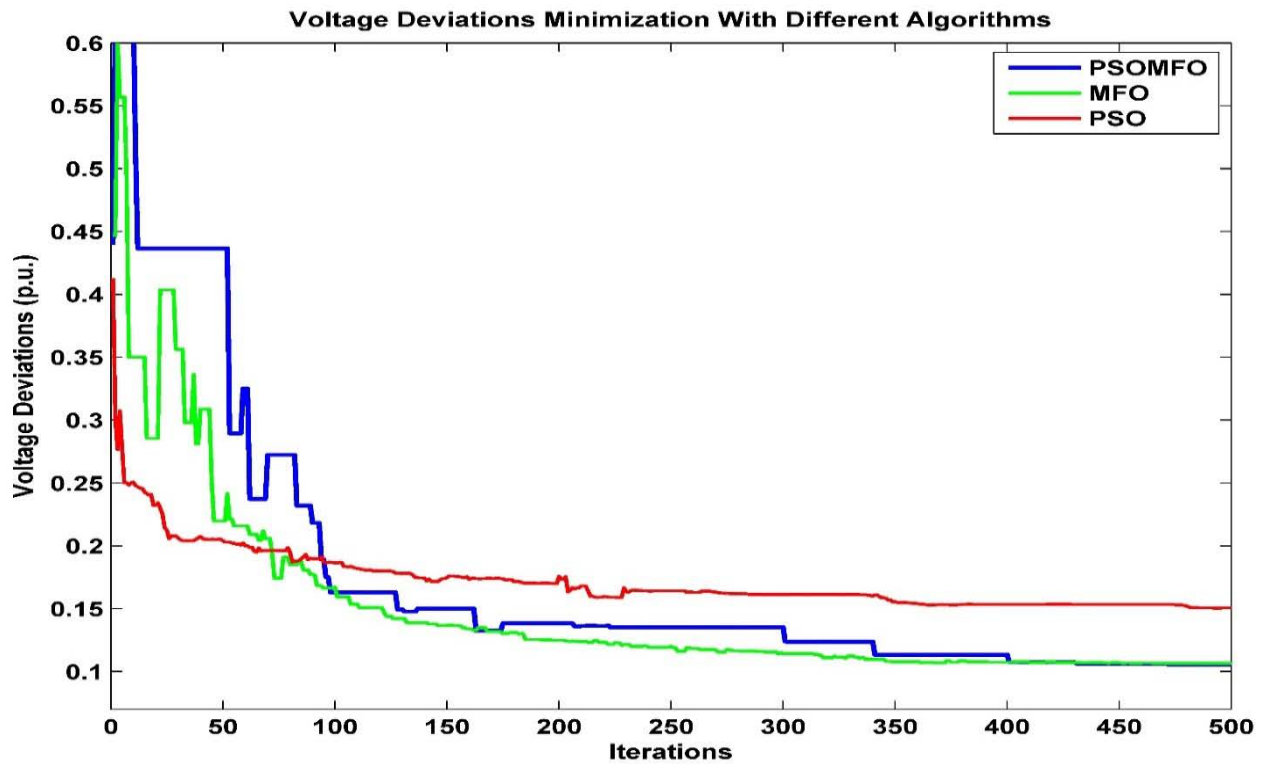


Fig. 4: Voltage deviation minimization with different algorithms

Table 4: Comparison of voltage deviations obtained with different algorithms

Method	Voltage Deviation (p.u)	Method Description
HPSO-MFO	0.1056	Hybrid Particle Swarm Optimization-Moth Flame Optimizer
MFO	0.1065	Moth Flame Optimizer
PSO	0.1506	Particle Swarm Optimization
GSA	0.0932	Gravitational Search Algorithm [2]
DE	0.1357	Differential Evolution [15]
BHBO	0.1262	Black Hole- Based Optimization [6]

Table 5: Optimal values of control variables for case 2 with different algorithms

Control Variable	Min	Max	Initial	HPSO-MFO	MFO	PSO
P_{G1}	50	200	99.2230	177.650	180.212	175.922
P_{G2}	20	80	80	49.092	49.584	46.389
P_{G5}	15	50	50	15.000	15.000	21.597
P_{G8}	10	35	20	10.000	24.349	19.396
P_{G11}	10	30	20	30.000	12.657	17.656
P_{G13}	12	40	20	12.000	12.000	12.000
V_{G1}	0.95	1.1	1.05	1.033	1.033	1.047
V_{G2}	0.95	1.1	1.04	1.017	1.017	1.034
V_{G5}	0.95	1.1	1.01	1.015	1.005	0.999
V_{G8}	0.95	1.1	1.01	0.997	0.999	1.005
V_{G11}	0.95	1.1	1.05	1.047	1.071	0.999
V_{G13}	0.95	1.1	1.05	1.016	1.052	1.018
T_{4-12}	0	1.1	1.078	1.065	1.100	0.954
T_{6-9}	0	1.1	1.069	0.914	0.900	0.969
T_{6-10}	0	1.1	1.032	0.973	1.072	0.989

T ₂₈₋₂₇	0	1.1	1.068	0.960	0.960	0.960
QC ₁₀	0	5	0	4.080	5.000	3.948
QC ₁₂	0	5	0	0.165	0.000	1.765
QC ₁₅	0	5	0	5.000	5.000	4.844
QC ₁₇	0	5	0	5.000	0.000	3.075
QC ₂₀	0	5	0	5.000	5.000	4.687
QC ₂₁	0	5	0	5.000	5.000	4.948
QC ₂₃	0	5	0	0.000	5.000	1.623
QC ₂₄	0	5	0	5.000	5.000	3.559
QC ₂₉	0	5	0	2.248	1.315	2.034
Vd	-	-	1.1496	0.1056	0.1065	0.1506

Case 3: Voltage stability enhancement

Presently, the transmission systems are enforced to work nearby their safety bounds, because of cost-effective and environmental causes. One of the significant characteristics of the system is its capability to retain continuously tolerable bus voltages to each node beneath standard operational environments, next to the rise in load, as soon as the system is being affected by disturbance. The unoptimized control variables may cause increasing and unmanageable voltage drop causing a tremendous voltage collapse [6]. Hence, voltage stability is inviting ever more attention. By using various techniques to evaluate the margin of voltage stability, Glavitch and Kessel have introduced a voltage stability index called L-index depends on the viability of load flow equations for every node [34]. The L-index of a bus shows the probability of voltage collapse circumstance for that particular bus. It differs between 0 and 1 equivalent to zero load and voltage collapse, respectively.

For the given system with NB , $N Gen$ and NLB buses signifying the total no. of buses, the total no. of generator buses and the total no. of load buses, respectively. The buses can be distinct as PV (generator) buses at the head and PQ (load) buses at the tail as follows [4]:

$$\begin{bmatrix} I_L \\ I_G \end{bmatrix} = [Y_{bus}] \begin{bmatrix} V_L \\ V_G \end{bmatrix} = \begin{bmatrix} Y_{LL} & Y_{LG} \\ Y_{GL} & Y_{GG} \end{bmatrix} \begin{bmatrix} V_L \\ V_G \end{bmatrix} \quad (39)$$

Where, Y_{LL} , Y_{LG} , Y_{GL} and Y_{GG} are co-matrix of Y_{bus} . The subsequent hybrid system of equations can be expressed as:

$$\begin{bmatrix} V_L \\ I_G \end{bmatrix} = [H] \begin{bmatrix} I_L \\ V_G \end{bmatrix} = \begin{bmatrix} H_{LL} & H_{LG} \\ H_{GL} & H_{GG} \end{bmatrix} \begin{bmatrix} I_L \\ V_G \end{bmatrix} \quad (40)$$

Where matrix H is produced by the partially inverting of Y_{bus} , H_{LL} , H_{LG} , H_{GL} and H_{GG} are the co-matrix of H , V_G , I_G , V_L and I_L are voltage and current vector of Generator buses and load buses, respectively.

The matrix H is given by:

$$[H] = \begin{bmatrix} Z_{LL} & -Z_{LL}Y_{LG} \\ Y_{GL}Z_{LL} & Y_{GG} - Y_{GL}Z_{LL}Y_{LG} \end{bmatrix} Z_{LL} = Y_{LL}^{-1} \quad (41)$$

Hence, the L-index denoted by L_j of bus j is represented as follows:

$$L_j = \left| 1 - \sum_{i=1}^{N_{Gen}} H_{LGji} \frac{v_i}{v_j} \right| \quad j=1,2,\dots,NL \quad (42)$$

Hence, the stability of the whole system is described by a global indicator L_{max} which is given by [6],

$$L_{max} = \max(L_j) \quad j=1,2,\dots,NL \quad (43)$$

The system is more stable as the value of L_{max} is lower.

The voltage stability can be enhanced by reducing the value of voltage stability indicator L -index at every bus of the system. [6].

Thus, the objective function may be given as follows:

$$Y = Y_{cost} + wY_{voltage_Stability_Enhancement} \quad (44)$$

$$\text{Where, } Y_{cost} = \sum_{i=1}^{N_{Gen}} f_i \quad (45)$$

$$Y_{voltage_stability_enhancement} = L_{max} \quad (46)$$

The variation of the L_{max} index with different algorithms over iterations is presented in fig. 4. The statistical results obtained with different methods are shown in table 6 which display that PSO-MFO method gives better results than the other methods. The optimal values of control variables obtained by different algorithms for case 3 are given in Table 7. After applying the PSO-MFO technique, it appears from Table 7 that the value of L_{max} is considerably decreased in this case compared to initial [6] from 0.1723 to 0.1126. Thus, the distance from breakdown point is improved.

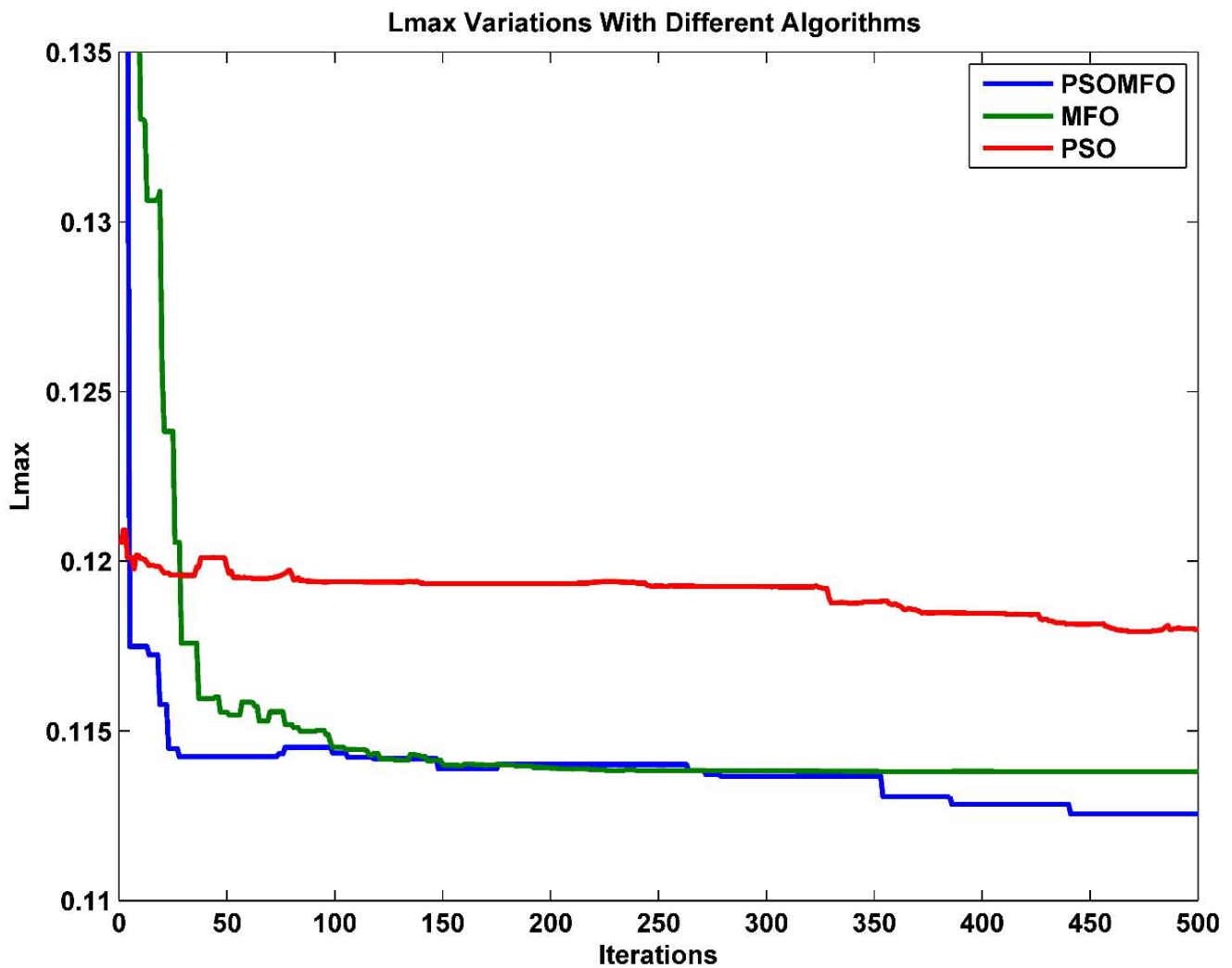


Fig. 5: L_{max} variations with different algorithms

Table 6: Comparison of L_{max} index obtained with different algorithms

Method	L_{max}	Method Description
HPSO-MFO	0.1126	Hybrid Particle Swarm Optimization-Moth Flame Optimizer
MFO	0.1138	Moth Flame Optimizer
PSO	0.1180	Particle Swarm Optimization
GSA	0.1162	Gravitational Search Algorithm [2]
DE	0.1219	Differential Evolution [15]
BHBO	0.1167	Black Hole- Based Optimization [6]

Table 7: Optimal values of control variables for case 3 with different algorithms

Control Variable	Min	Max	Initial	HPSO-MFO	MFO	PSO
P_{G1}	50	200	99.2230	182.308	177.299	158.331
P_{G2}	20	80	80	45.360	48.792	49.050
P_{G5}	15	50	50	21.109	21.316	18.956
P_{G8}	10	35	20	21.557	20.351	31.224
P_{G11}	10	30	20	10.000	12.370	15.906
P_{G13}	12	40	20	12.000	12.012	17.801
V_{G1}	0.95	1.1	1.05	1.100	1.100	1.098

V_{G2}	0.95	1.1	1.04	1.086	1.089	1.090
V_{G5}	0.95	1.1	1.01	1.063	1.063	1.043
V_{G8}	0.95	1.1	1.01	1.077	1.055	1.058
V_{G11}	0.95	1.1	1.05	1.100	1.100	1.081
V_{G13}	0.95	1.1	1.05	1.098	1.100	1.100
T_{4-12}	0	1.1	1.078	1.034	0.996	0.900
T_{6-9}	0	1.1	1.069	0.900	0.900	1.007
T_{6-10}	0	1.1	1.032	0.973	0.964	1.071
T_{28-27}	0	1.1	1.068	0.968	0.955	0.933
QC_{10}	0	5	0	5.000	5.000	3.286
QC_{12}	0	5	0	5.000	5.000	1.221
QC_{15}	0	5	0	5.000	5.000	4.601
QC_{17}	0	5	0	5.000	5.000	1.082
QC_{20}	0	5	0	5.000	5.000	0.444
QC_{21}	0	5	0	5.000	5.000	0.399
QC_{23}	0	5	0	5.000	5.000	2.446
QC_{24}	0	5	0	5.000	5.000	4.753
QC_{29}	0	5	0	5.000	4.984	3.887
L_{max}	-	-	0.1723	0.1126	0.1138	0.1180

Case 4: Minimization of active power transmission losses

In the case 4 the Optimal Power Flow objective is to reduce the active power transmission losses, which can be represented by power balance equation as follows [6]:

$$J = \sum_{i=1}^{N_{Gen}} P_i = \sum_{i=1}^{N_{Gen}} P_{Gi} - \sum_{i=1}^{N_{Gen}} P_{Di} \quad (47)$$

Fig. 5 show the tendency for reducing the total real power losses objective function using the different techniques. The active power losses obtained with

different techniques are shown in table 8 which made sense that the results obtained by PSO-MFO give better values than the other methods. The optimal values of control variables obtained by different algorithms for case 4 are displayed in Table 9. By means of the same settings the results achieved in case 4 with the PSO-MFO technique are compared to some other methods and it display that the real power transmission losses are greatly reduced compared to the initial case [6] from 5.821 MW to 2.831 MW.

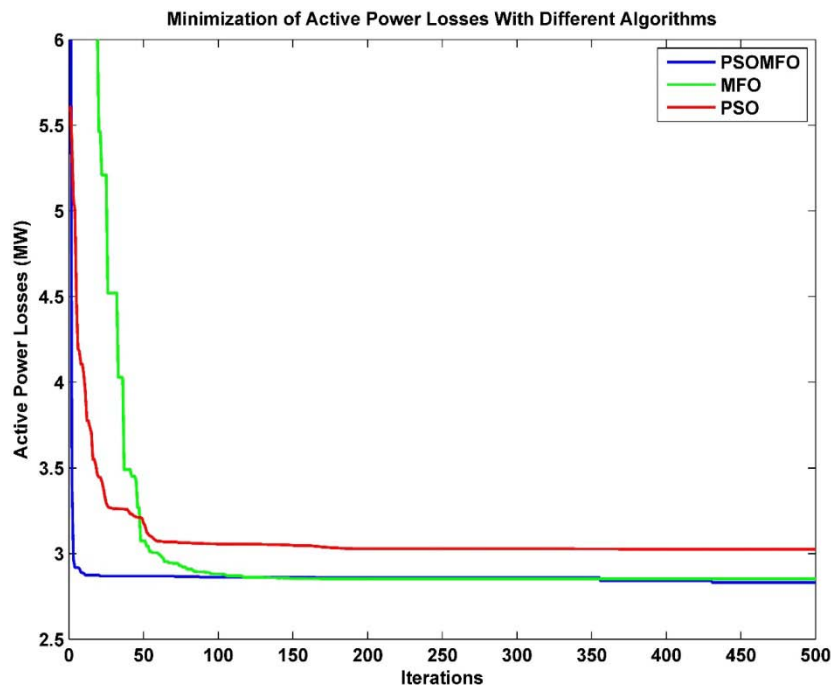


Fig. 6: Minimization of active power losses with different algorithms

Table 8: Comparison of active power transmission losses obtained with different algorithms

Method	Active Power Loss (MW)	Method Description
HPSO-MFO	2.831	Hybrid Particle Swarm Optimization-Moth Flame Optimizer
MFO	2.853	Moth Flame Optimizer
PSO	3.026	Particle Swarm Optimization
BHBO	3.503	Black Hole- Based Optimization [6]

Table 9: Optimal values of control variables for case 4 with different algorithms

Control Variable	Min	Max	Initial	HPSO-MFO	MFO	PSO
P_{G1}	50	200	99.2230	51.269	51.253	51.427
P_{G2}	20	80	80	80.000	80.000	80.000
P_{G5}	15	50	50	50.000	50.000	50.000
P_{G8}	10	35	20	35.000	35.000	35.000
P_{G11}	10	30	20	30.000	30.000	30.000
P_{G13}	12	40	20	40.000	40.000	40.000
V_{G1}	0.95	1.1	1.05	1.100	1.100	1.100
V_{G2}	0.95	1.1	1.04	1.100	1.098	1.100
V_{G5}	0.95	1.1	1.01	1.082	1.080	1.083
V_{G8}	0.95	1.1	1.01	1.086	1.087	1.090
V_{G11}	0.95	1.1	1.05	1.100	1.100	1.100
V_{G13}	0.95	1.1	1.05	1.100	1.100	1.100
T_{4-12}	0	1.1	1.078	1.044	1.056	0.977
T_{6-9}	0	1.1	1.069	0.901	0.900	1.100
T_{6-10}	0	1.1	1.032	0.993	0.982	1.100
T_{28-27}	0	1.1	1.068	0.987	0.973	0.998
QC_{10}	0	5	0	5.000	5.000	4.065
QC_{12}	0	5	0	4.570	5.000	0.000
QC_{15}	0	5	0	4.969	3.070	5.000
QC_{17}	0	5	0	4.942	5.000	5.000
QC_{20}	0	5	0	4.337	5.000	0.000
QC_{21}	0	5	0	5.000	5.000	5.000
QC_{23}	0	5	0	5.000	5.000	5.000
QC_{24}	0	5	0	5.000	5.000	0.000
QC_{29}	0	5	0	2.412	2.508	0.000
P Loss (MW)	-	-	5.8219	2.831	2.853	3.026

Case 5: Minimization of reactive power transmission losses

The accessibility of reactive power is the main point for static system voltage stability margin to support the transmission of active power from the source to sinks [6].

Thus, the minimization of VAR losses are given by the following expression:

$$J = \sum_{i=1}^{N_{Gen}} Q_i = \sum_{i=1}^{N_{Gen}} Q_{Gi} - \sum_{i=1}^{N_{Gen}} Q_{Di} \quad (48)$$

It is notable that the reactive power losses are not essentially positive. The variation of reactive power losses with different methods shown in fig. 6. It demonstrates that the suggested method has good convergence characteristics. The statistical values of reactive power losses obtained with different methods are shown in table 10 which display that the results obtained by hybrid PSO-MFO method are better than the other methods. The optimal values of control variables obtained by different algorithms for case 5 are

given in Table 11. It is shown that the reactive power losses are greatly reduced compared to the initial case [6] from -4.6066 MVAR to -25.335MVAR using hybrid PSO-MFO method.

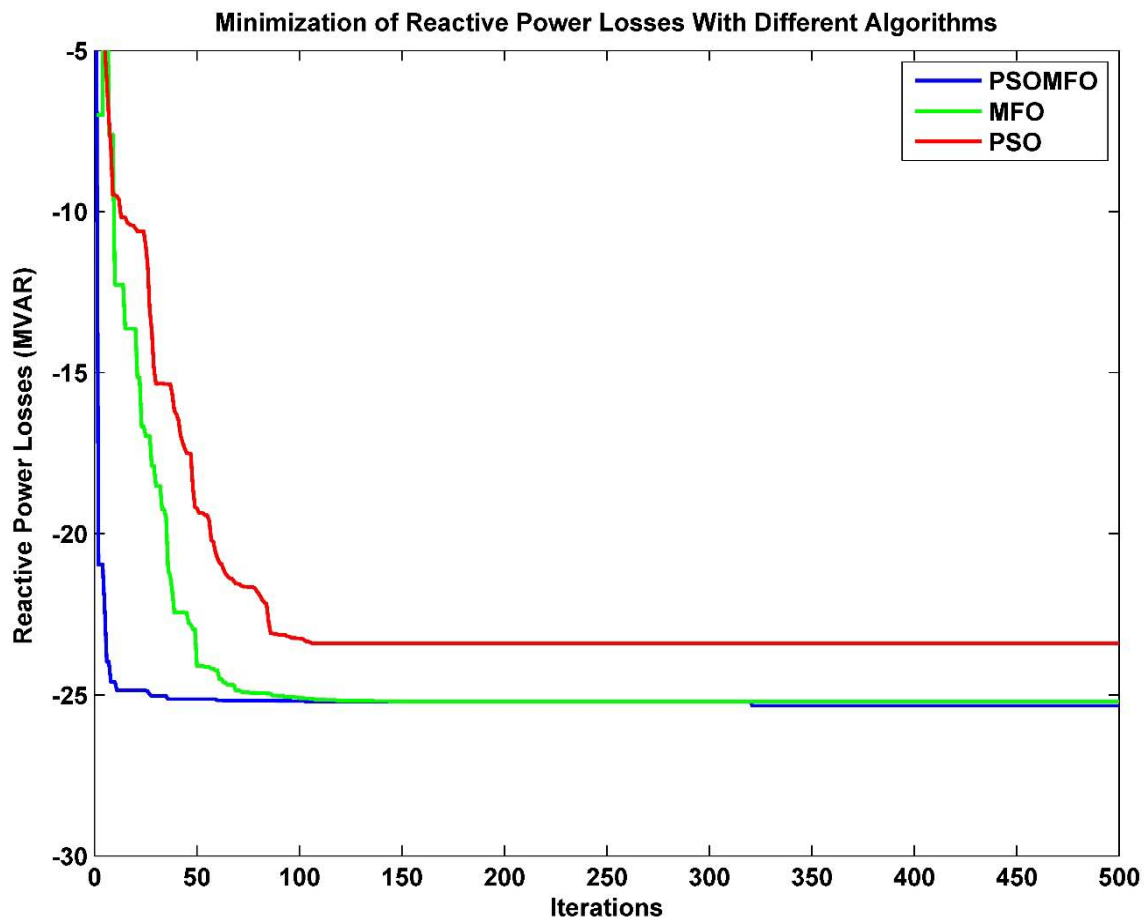


Fig. 7: Minimization of reactive power transmission losses with different algorithms

Table 10: Comparison of reactive power losses obtained with different algorithms

Method	Reactive Power Loss (MVAR)	Method Description
HPSO-MFO	-25.335	Hybrid Particle Swarm Optimization-Moth Flame Optimizer
MFO	-25.204	Moth Flame Optimizer
PSO	-23.407	Particle Swarm Optimization
BHBO	-20.152	Black Hole- Based Optimization [6]

Table 11: Optimal values of control variables for case 5 with different algorithms

Control Variable	Min	Max	Initial	HPSO-MFO	MFO	PSO
P_{G1}	50	200	99.2230	51.318	51.356	51.644
P_{G2}	20	80	80	80.000	80.000	80.000
P_{G5}	15	50	50	50.000	50.000	50.000
P_{G8}	10	35	20	35.000	35.000	35.000
P_{G11}	10	30	20	30.000	30.000	30.000
P_{G13}	12	40	20	40.000	40.000	40.000
V_{G1}	0.95	1.1	1.05	1.100	1.100	1.100
V_{G2}	0.95	1.1	1.04	1.100	1.100	1.100
V_{G5}	0.95	1.1	1.01	1.092	1.092	1.100
V_{G8}	0.95	1.1	1.01	1.100	1.100	1.100
V_{G11}	0.95	1.1	1.05	1.100	1.100	1.100
V_{G13}	0.95	1.1	1.05	1.100	1.100	1.100
T_{4-12}	0	1.1	1.078	1.002	0.974	0.962
T_{6-9}	0	1.1	1.069	0.965	1.100	1.100
T_{6-10}	0	1.1	1.032	0.987	0.984	0.961

T_{28-27}	0	1.1	1.068	0.986	0.981	0.964
QC ₁₀	0	5	0	5.000	5.000	5.000
QC ₁₂	0	5	0	0.000	5.000	0.000
QC ₁₅	0	5	0	5.000	5.000	0.000
QC ₁₇	0	5	0	5.000	5.000	0.000
QC ₂₀	0	5	0	5.000	5.000	0.000
QC ₂₁	0	5	0	5.000	5.000	0.000
QC ₂₃	0	5	0	5.000	5.000	0.000
QC ₂₄	0	5	0	5.000	5.000	5.000
QC ₂₉	0	5	0	3.393	3.407	0.000
QLoss (MVAR)	-	-	-4.6066	-25.335	-25.204	-23.407

Table 12 show the comparison of elapsed time taken by the different methods to optimize the different objective cases. The comparison shows that the time taken by all three algorithms is not same which indicates the different evaluation strategy of different methods.

Table 12: Comparison of Elapsed time in seconds for MFO, PSO and HPSO-MFO for all cases

Case No.	Elapsed Time (Seconds)		
	MFO	PSO	HPSO-MFO
1	166.2097	250.2674	211.7915
2	191.8238	266.5375	229.6873
3	196.6275	270.3358	243.2919
4	161.6395	248.8739	259.9731
5	173.5987	253.3971	209.4387

V. ROBUSTNESS TEST

In order to check the robustness of the HPSO-MFO for solving continues Optimal Power Flow problems, 10 times trials with various search agents for cases Case 1, Case 2, Case 3, Case 4 and Case 5. Table 2, Table 3, Table 4, Table 5, Table 6, Table 7, Table 8, Table 9, Table 10 and Table 11 presents the statistical results achieved by the HPSO-MFO, MFO and PSO algorithms for OPF problems for various cases. From these tables, it is clear that the optimum objective function values obtained by HPSO-MFO are near to every trial and minimum compare to MFO and PSO algorithms. It proves the robustness of hybrid PSO-MFO algorithm (HPSO-MFO) to solve OPF problem.

VI. CONCLUSION

Particle Swarm Optimization-Moth Flame Optimizer (PSO-MFO), Moth Flame Optimizer and Particle Swarm Optimization Algorithm are successfully applied to standard IEEE 30-bus test systems to solve the optimal power flow problem for the various types of cases. The results give the optimal settings of control variables with different methods which demonstrate the effectiveness of the different techniques. The solutions obtained from the hybrid PSO-MFO method approach has good convergence characteristics and gives the better results compared to MFO and PSO methods which confirm the effectiveness of proposed algorithm.

VII. ACKNOWLEDGMENT

The authors would like to thank Professor Seyedali Mirjalili for his valuable comments and support. <http://www.alimirjalili.com/MFO.html>.

REFERENCES RÉFÉRENCES REFERENCIAS

- H.R.E.H. Boucekara, M.A. Abido, A.E. Chaib, R. Mehasni, Optimal power flow using the league championship algorithm: a case study of the Algerian power system, *Energy Convers. Manag.* 87 (2014) 58–70.
- Duman S, Güvenç U, Sönmez Y, Yörükeren N. Optimal power flow using gravitational search algorithm. *Energy Convers Manag*2012; 59:86–95.
- Niknam T, R Narimani M, Jabbari M, Malekpour AR. A modified shuffle frog-leaping algorithm for multi-objective optimal power flow. *Energy* 2011; 36(11): 6420–32.
- J. Carpentier, Contribution à l'étude du Dispatching Economique, *Bull. Soc. Fran-caise Electriciens* (1962) 431–447.
- H.R.E.H. Boucekara, M.A. Abido, M. Boucherma, Optimal power flow using Teaching-Learning-Based Optimization technique, *Electr. Power Syst. Res.* 114(2014) 49–59.
- H.R.E.H. Boucekara, Optimal power flow using black-hole-based optimization approach, *Appl. Soft Comput.* (2013) (under review).
- S. Frank, I. Steponavice, S. Rebennack, Optimal power flow: a bibliographicsurvey I, formulations

- and deterministic methods, *Energy Syst.* 3 (3) (2012)221–258.
8. M.R. AlRashidi, M.E. El-Hawary, Applications of computational intelligence techniques for solving the revived optimal power flow problem, *Electr. Power Syst. Res.* 79 (4) (2009) 694–702.
 9. S. Frank, I. Steponavice, S. Rebennack, Optimal power flow: a bibliographic survey II, non-deterministic and hybrid methods, *Energy Syst.* 3 (3) (2012)259–289.
 10. A.R. Yildiz, A comparative study of population-based optimization algorithms for turning operations, *Inf. Sci. (Ny)* 210 (2012) 81–88.
 11. LJ Cai, I Erlich and G Stamtzis. Optimal choice and allocation of FACTS devices in deregulated electricity market using genetic algorithms. *IEEE.* 2004.
 12. TS Chung and YZ Li. A hybrid GA approach for OPF with consideration of FACTS devices. *IEEE Power Engineering Review.* 2001; 47-50.
 13. K Kalaiselvi, V Kumar, and K Chandrasekar. Enhanced Genetic Algorithm for Optimal Electric Power Flow using TCSC and TCPS. *Proc. World.* 2010; (II).
 14. AG Bakirtzis. P Biskas, CE Zoumas, and V Petridis. Optimal power flow by enhanced genetic algorithm. *Power Syst, IEEE Trans.* 2002; 17(2): 229–236.
 15. A.A. Abou El Ela, M.A. Abido, Optimal power flow using differential evolution algorithm, *Electr. Power Syst. Res.* 80 (7) (2010) 878–885.
 16. Slimani L, Bouktir T. Optimal Power Flow Solution of the Algerian Electrical Network using Differential Evolution Algorithm. *TELKOMNIKA Indonesian Journal of Electrical Engineering.* 2012; 10(2): 199–210.
 17. Badrul H Chowdhury. Towards the concept of integrated security: optimal dispatch under static and dynamic security constraints. *Electric Power Syst, Research.*1992; 25: 213-225.
 18. M Saravanan, SM Slochanal, P Venkatesh, J Abraham. Application of particle swarm optimization technique for optimal location of FACTS devices considering cost of installation and system loadability. *Electric Power Syst, Research.* 2007; 77: 276-283.
 19. Abido MA. Optimal power flow using tabu search algorithm. *Electric Power Compon Syst.* 2002; 30: 469–83.
 20. S Duman U Güvenç, Y Sönmez and N Yörükeren. Optimal power flow using gravitational search algorithm. *Energy Convers, Manag.* 2012; 59: 86–95.
 21. A Bhattacharya and PChattopadhyay. Application of biogeography-based optimisation to solve different optimal power flow problems. *IET Gener, Transm. Distrib.* 2011; 5(1): 70.
 22. N Sinsupan, U Leeton and T Kulworawanichpong. *Application of Harmony Search to Optimal Power Flow Problems.* 2010:219–222.
 23. A Mukherjee and V Mukherjee. *Solution of optimal power flow using chaotic krill herd algorithm.* *Chaos, Solitons & Fractals.* 2015; 78: 10–21.
 24. M Rama, Mohana Rao and AV NareshBabu. Optimal Power Flow Using Cuckoo Optimization Algorithm. *IJAREEIE.* 2013: 4213–4218.
 25. J Soares. T Sousa. ZA Vale. H Morais. and P Faria. Ant colony search algorithm for the optimal power flow problem. *IEEE Power Energy Soc, Gen, Meet.* 2011; 1–8.
 26. Indrajit N. Trivedi, Motilal Bhoje, Pradeep Jangir, Siddharth A. Parmar, Narottam Jangir and Arvind Kumar, "Voltage stability enhancement and voltage deviation minimization using BAT optimization algorithm," *2016 3rd International Conference on Electrical Energy Systems (ICEES)*, Chennai, India, 2016, pp. 112-116. doi: 10.1109/ICEES.2016.7510626.
 27. Optimal power flow with enhancement of voltage stability and reduction of power loss using ant-lion optimizer, Indrajit N. Trivedi, Pradeep Jangir & Siddharth A. Parmar, *Cogent Engineering* (2016), 3: 1208942.
 28. Indrajit N. Trivedi, Siddharth A. Parmar, R.H. Bhesdadiya, Pradeep Jangir, "Voltage stability enhancement and voltage deviation minimization using Ant-Lion optimizer algorithm", *2016 2nd International Conference on Advances in Electrical, Electronics, Information, Communication and Bio-Informatics (AEEICB)*, Chennai, India, 2016, pp. 263-267. doi: 10.1109/AEEICB.2016.7538286.
 29. Indrajit N. Trivedi, Pradeep Jangir, Narottam Jangir, Siddharth A. Parmar, Motilal Bhoje and Arvind Kumar, "Voltage stability enhancement and voltage deviation minimization using Multi-Verse optimizer algorithm," *2016 International Conference on Circuit, Power and Computing Technologies (ICCPCT)*, Nagercoil, India, 2016, pp. 1-5. doi: 10.1109/ICCPCT.2016.7530136.
 30. J. Kennedy, R. Eberhart, Particle swarm optimization, in: *Proceedings of the IEEE International Conference on Neural Networks*, Perth, Australia, 1995, pp. 1942–1948.
 31. Seyedali Mirjalili, "Moth-flame optimization algorithm: A novel nature-inspired heuristic paradigm," *Knowledge-Based System*, vol. 89, pages 228-249, 2015.
 32. Narottam Jangir, Mahesh H. Pandya, Indrajit N. Trivedi, R. H. Bhesdadiya, Pradeep Jangir and Arvind Kumar, "Moth-Flame optimization Algorithm for solving real challenging constrained engineering optimization problems," *2016 IEEE Students' Conference on Electrical, Electronics and Computer*

- Science (SCEECS)*, Bhopal, India, 2016, pp. 1-5. doi: 10.1109/SCEECS.2016.7509293.
33. K. Lee, Y. Park, J. Ortiz, A united approach to optimal real and reactive power dispatch, *IEEE Trans. Power App. Syst.* 104 (5) (1985) 1147–1153.
 34. P. Kessel, H. Glavitsch, Estimating the voltage stability of a power system, *IEEETrans. Power Deliv.* 1 (3) (1986) 346–354.
 35. W. Ongsakul, T. Tantimaporn, Optimal power flow by improved evolutionary programming, *Electr. Power Compon. Syst.* 34 (1) (2006) 79–95.
 36. C.A. Belhadj, M.A. Abido, An optimized fast voltage stability indicator, in: *Electric Power International Conference on Engineering*, Power Tech Budapest, 1999, pp. 79–83.
 37. S.A.H. Soliman, A.H. Mantawy, *Modern Optimization Techniques with Applications in Electric Power Systems*, Energy Systems, Springer, New York/Heidelberg/Dordrecht/London, 2012.

